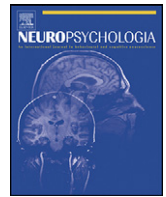




Contents lists available at ScienceDirect

## Neuropsychologia

journal homepage: [www.elsevier.com/locate/neuropsychologia](http://www.elsevier.com/locate/neuropsychologia)

## Experience-dependent plasticity of white-matter microstructure extends into old age

Martin Lövdén<sup>a,b,c,\*</sup>, Nils Christian Bodammer<sup>a,d</sup>, Simone Kühn<sup>e,f</sup>, Jörn Kaufmann<sup>d</sup>, Hartmut Schütze<sup>d</sup>, Claus Tempelmann<sup>d</sup>, Hans-Jochen Heinze<sup>d,i</sup>, Emrah Düzel<sup>d,g,i</sup>, Florian Schmiedek<sup>a,h</sup>, Ulman Lindenberger<sup>a</sup>

<sup>a</sup> Center for Lifespan Psychology, Max Planck Institute for Human Development, Berlin, Germany

<sup>b</sup> Department of Psychology, Lund University, Sweden

<sup>c</sup> Aging Research Center (ARC), Karolinska Institutet and Stockholm University, Stockholm, Sweden

<sup>d</sup> Department of Neurology, Otto-von-Guericke University Magdeburg, Germany

<sup>e</sup> Department of Psychology, Max Planck Institute for Human Cognitive and Brain Sciences, Germany

<sup>f</sup> Department of Experimental Psychology, Ghent University, Belgium

<sup>g</sup> Institute of Cognitive Neuroscience, University College London, UK

<sup>h</sup> German Institute for International Educational Research (DIPF), Frankfurt am Main, Germany

<sup>i</sup> DZNE (German Centre for Neurodegenerative Disorders), Magdeburg, Germany

## ARTICLE INFO

## Article history:

Received 20 April 2010

Received in revised form 25 August 2010

Accepted 27 August 2010

Available online 15 September 2010

## Keywords:

Aging

Cognitive training

Plasticity

White-matter microstructure

## ABSTRACT

Experience-dependent alterations in the human brain's white-matter microstructure occur in early adulthood, but it is unknown whether such plasticity extends throughout life. We used cognitive training, diffusion-tensor imaging (DTI), and structural MRI to investigate plasticity of the white-matter tracts that connect the left and right hemisphere of the frontal lobes. Over a period of about 180 days, 20 younger adults and 12 older adults trained for a total of one hundred and one 1-h sessions on a set of three working memory, three episodic memory, and six perceptual speed tasks. Control groups were assessed at pre- and post-test. Training affected several DTI metrics and increased the area of the anterior part of the corpus callosum. These alterations were of similar magnitude in younger and older adults. The findings indicate that experience-dependent plasticity of white-matter microstructure extends into old age and that disruptions of structural interhemispheric connectivity in old age, which are pronounced in aging, are modifiable by experience and amenable to treatment.

© 2010 Elsevier Ltd. All rights reserved.

Several findings indicate that the brain's white-matter displays experience-dependent changes in adulthood (Fields, 2008). For example, neural activity can induce myelination (Demerens et al., 1996; Stevens, Porta, Haak, Gallo, & Fields, 2002) and rhesus monkeys raised in enriched environments display larger corpus callosum size and improved cognitive performance (Sanchez, Hearn, Do, Rilling, & Herndon, 1998). In humans, amount of piano practicing in childhood and early adulthood correlates with white-matter microstructure as observed with diffusion-tensor imaging (DTI; Bengtsson et al., 2005) and young adults practicing juggling show microstructural changes in white-matter (Scholz, Klein, Behrens, & Johansen-Berg, 2009). Considering that impairments in white-matter integrity are pronounced in aging (for reviews, see Madden,

Bennett, & Song, 2009; Sullivan & Pfefferbaum, 2006), it is important to examine whether such plasticity extends into old age, and thus whether adult age-related differences in white-matter integrity are modifiable by experience and amenable to treatment.

We investigated the plasticity of white-matter microstructure in younger and older adulthood with a cognitive intervention (Schmiedek, Lövdén, & Lindenberger, 2010). Twenty younger and 12 older adults participated in the intervention, which consisted of an average of one hundred and one 1-h training sessions, each comprising practice on 12 different cognitive tasks, three related to working memory, three to episodic memory, and six to perceptual speed. Pretests and posttests conducted before and after training included DTI, which assess white-matter microstructure by quantifying free diffusion of water (mean diffusivity) as well as the directional rate (anisotropy) of water diffusion. Control groups took part in identical DTI measurements.

In this study, we were particularly interested in the white-matter tracts that connect the prefrontal cortices. These tracts are located in the anterior part of the corpus callosum (i.e., genu; see

\* Corresponding author at: Center for Lifespan Psychology, Max Planck Institute for Human Development, Lentzeallee 94, 14195 Berlin, Germany.  
Tel.: +49 30 82406 216.

E-mail address: [loevden@mpib-berlin.mpg.de](mailto:loevden@mpib-berlin.mpg.de) (M. Lövdén).

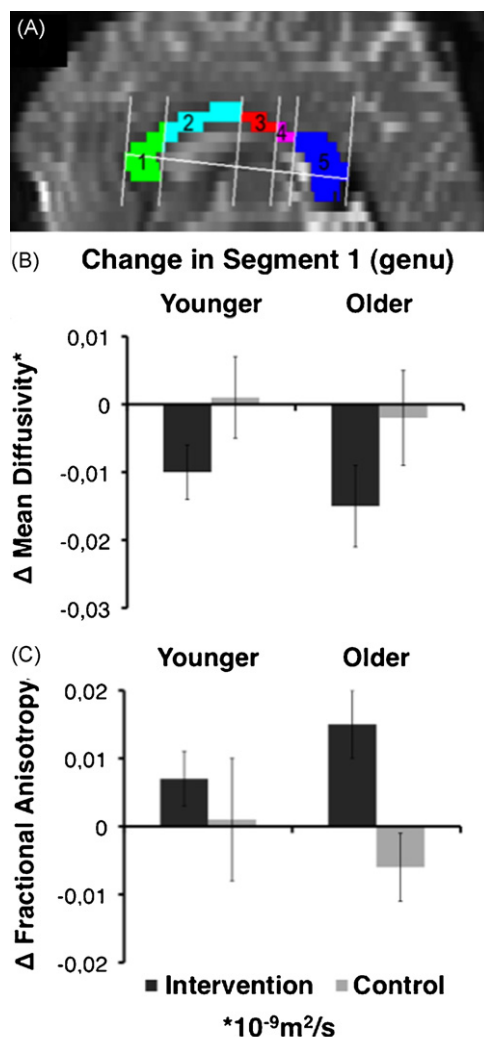


**Fig. 1.** (A) Midsagittal slice of a MD dataset showing corpus callosum sub-segmented (Hofer & Frahm, 2006) into regions likely connecting the prefrontal (1; genu), premotor and supplementary motor (2), motor (3), sensory (4), and temporal, parietal, and occipital (5; splenium) cortices. (B) Mean change ( $\Delta$ ;  $\pm$ SE) from pretest to posttest in mean diffusivity, and (C) fractional anisotropy in segment 1 (genu) of the corpus callosum as a function of age and experimental group.

Fig. 1A). This region shows more pronounced age-related decline than more posterior regions of the corpus callosum (Burzynska et al., 2010; Sullivan & Pfefferbaum, 2006). In addition, these age-related differences in structural connectivity can account for age differences in cognitive performance (Madden, Spaniol, et al., 2009) and functional brain activation (Persson et al., 2006; Sullivan & Pfefferbaum, 2006). Thus, from the perspective of aging research it is highly relevant to investigate the possibility of experience-dependent changes of the white-matter tracts connecting the prefrontal cortices. Notably, most of the cognitive tasks used in our intervention are known to activate the prefrontal cortices (Cabeza & Nyberg, 2000) and impose high attentional control demands that require interhemispheric communication (Banich, 1998; Mikels & Reuter-Lorenz, 2004). Thus, it makes sense to predict that that our intervention should affect the structural integrity of the tracts that connect the prefrontal cortices, although the prefrontal cortices are not the only brain regions activated by the tasks included in the intervention. We therefore first segmented the whole the corpus callosum on the pre- and post-test diffusion-tensor images from each participant with a semi-automatic technique (Niogi, Mukherjee, & McCandliss, 2007). Based on the geometric scheme

proposed by Hofer and Frahm (2006), we then further divided the corpus callosum into segments likely connecting the prefrontal (segment 1; genu), premotor and supplementary motor (2), motor (3), sensory (4), and temporal, parietal, and occipital (5; splenium) cortices (see Fig. 1A). For each segment, we then obtained the mean value of the fractional anisotropy (FA) index, which reflects the anisotropy of water diffusion in tissue due to the hindrance of membranes and therefore is partly dependent on density and orientational coherence of white-matter tracts, and the average value of the mean diffusivity (MD), which reflects the degree to which diffusion of water is free – without considering orientation – and therefore serves as a measure for barrier sparseness. The segment-specific FA means and MD means were used as primary dependent variables from the DTI data.

## 1. Materials and methods

### 1.1. Participants

Participants were recruited through newspaper advertisements, word-of-mouth recommendation, and flyers circulated in Berlin, Germany, for a longitudinal study (COGITO) on day-to-day variability of cognitive performance. This parent study involved 101 younger (aged 20–31 years) and 103 older adults (aged 65–80 years) completing an average of 101 daily sessions of cognitive assessment. These participants were also invited to, and 30 younger and 27 older eligible volunteers were recruited for, diffusion tensor imaging (DTI) planned to take place before (pretest) and after (posttest) the cognitive intervention phase. Younger ( $n = 11$ ) and older ( $n = 13$ ) control groups were recruited to take part in imaging only. All participants were right-handed, had normal or corrected-to-normal vision, and reported no history of cardiovascular disease (except treated hypertension), diabetes, neurological or psychiatric conditions, or drug/alcohol abuse. They reported no use of anti-seizure or anti-depressant drugs. Older participants were screened for dementia using the mini-mental state examination (MMSE; Folstein, Folstein, & McHugh, 1975) with a cut-off of 26.

Based on evaluations by a clinical neurologist, one younger and six older intervention participants were excluded at pretest due to various brain abnormalities as observed on structural (T1) images. Due to technical failures or imaging artefacts (e.g., movement) at pretest, DTI data were lost for five younger and seven older intervention participants. Four younger and two older intervention participants dropped out during the longitudinal phase of the study. In the control groups, one younger adult dropped out between pretest and posttest.

Thus, the effective sample for this article consisted of 20 younger (11 women;  $M_{\text{age}} = 25.1$ ;  $SD = 2.8$ ; range = 20–30 years) and 12 older (7 women;  $M_{\text{age}} = 68.9$ ;  $SD = 2.7$ ; range = 65–75 years) adults in intervention groups and 10 younger (4 women;  $M_{\text{age}} = 25.6$ ;  $SD = 2.6$ ; range = 22–30 years) and 13 older (4 women;  $M_{\text{age}} = 69.7$ ;  $SD = 3.5$ ; range = 65–76 years) adults in control groups. Intervention groups and control groups were statistically comparable on chronological age [ $t(28) = 0.45$ , for young;  $t(23) = 0.58$ , for old], vocabulary (Lindenberger, Mayr, & Kliegl, 1993; cf. Lehrl, Merz, Burkard, & Fischer, 1991) scores assessed at pretest [ $t(28) = 0.64$ , for young;  $t(23) < 0.01$ , for old], and MMSE scores [ $t(23) < 0.60$ , for old]. Four older intervention participants and one older control participant were treated for hypertension.

Participants in the intervention groups were paid between 1450 and 1950€, depending on the number of completed sessions and their pace of completing the longitudinal phase of the study. Participants in the control groups were paid 200€. All participants gave written informed consent to participate. The ethical review board of the Otto-von-Guericke University of Magdeburg approved the imaging sub-study and the review board of Max Planck for Human Development, Berlin, approved the behavioral parent study.

### 1.2. Training procedures

During the longitudinal practice phase, intervention groups practiced three working memory, three episodic memory, and six perceptual speed tasks during on average one hundred and one ( $M_{\text{young}} = 102$ ,  $SD_{\text{young}} = 3.3$ ;  $M_{\text{old}} = 100$ ,  $SD_{\text{old}} = 3.7$ ) 1-h sessions. Participants practiced individually in lab rooms containing up to six computerized testing stations. In addition, intervention groups completed behavioral pretests and posttests during ten sessions that consisted of 2–2.5 h of cognitive test batteries and self-report questionnaires (e.g., personality inventories). A pretest brain-imaging session was conducted after the behavioral pretest and immediately before the longitudinal practice phase. The posttest imaging session was completed shortly after the completion of the behavioral posttest. The imaging sessions were separated by an average of 179 days ( $M_{\text{young}} = 183$ ,  $SD_{\text{young}} = 21.0$ ;  $M_{\text{old}} = 173$ ,  $SD_{\text{old}} = 25.2$ ). The control groups took part in imaging pretests and posttests only, which were separated by an average of 186 days ( $M_{\text{young}} = 189$ ,  $SD_{\text{young}} = 8.6$ ;  $M_{\text{old}} = 184$ ,  $SD_{\text{old}} = 15.0$ ).

The tasks practiced by the intervention groups were administered with several stimuli–presentation times at pretest. This procedure allowed for estimation of time–accuracy functions, which describe a person's accuracy as a function of presentation time. To maximize and even out the cognitive challenge of these tasks across individuals, while also maintaining motivation, the time–accuracy information was used for tailoring the difficulty of the subsequently practiced tasks by adjusting presentation time for each individual at the start of the intervention. Presentation times were kept constant over the intervention period. The practiced tasks are described in detail in the section below. Performance at pretest and posttest assessments, collapsed over presentation times, were used as dependent variables.

#### 1.2.1. Spatial working memory: 3-Back

A sequence of 39 black dots appeared at varying locations in a 4 by 4 grid. Participants had to respond to each dot as to whether it was in the same position as the dot three steps earlier in the sequence or not. Four blocks were included in each daily session.

#### 1.2.2. Numerical working memory: Memory updating

In each of four horizontally placed cells, four single digits (in the range of 0–9) were presented simultaneously for 4000 ms. After an ISI of 500 ms, eight updating operations were presented sequentially in a second row at varying horizontal position. The requested updating operations were additions and subtractions in the range of –8 to +8. Those updating operations had to be applied to the memorized digits from the corresponding cells above and the updated results had to be memorized. At the end of each trial, the four end results had to be entered in the four cells in the upper row. Eight blocks were included in each daily session.

#### 1.2.3. Verbal working memory: Alpha span

Ten upper-case consonant letters were presented sequentially, together with a number below the letter. For each letter, participants had to decide as quickly as possible whether the number corresponds to the alphabetic position of the current letter within the set of letters presented up to this step. Five of the ten items were targets. Eight blocks were included in each daily session.

#### 1.2.4. Figural–spatial episodic memory: Object–position memory

Sequences of 12 coloured photographs of real-world objects were displayed at different locations in a 6 × 6 grid, which thus contained 36 possible screen-locations at which an object could be presented for encoding. After this presentation phase, the objects appeared at the bottom of the screen (below the 6 × 6 grid) and had to be moved in the order of which they were presented during encoding to the correct locations, by clicking on objects and locations with the computer mouse. Two blocks were included in each daily session.

#### 1.2.5. Numerical episodic memory: Number–noun pairs

Lists of 12 two-digit numbers and nouns in plural case pairs were presented sequentially. After presentation, all numbers had to be entered prompted in random order by the nouns. Two blocks were included in each daily session.

#### 1.2.6. Verbal episodic memory: Word lists

Lists of 36 nouns were presented sequentially. After presentation, the first three letters of each word had to be entered in correct order using the keyboard. Two blocks were included in each daily session.

#### 1.2.7. Perceptual speed: Choice reaction tasks (CRT)

Three CRTs were based on the same stimulus layout, the seven lines of the number “8” as displayed on pocket calculators. Stimuli were masked with a stimulus that combined this “calculator 8” with extending lines in all 10 possible directions. Possible masking times were 1, 2, 4, or 8 screen cycles (12, 24, 47, or 94 ms). Depending on pretest performance, two out of these masking times (one fast and one slow condition) were chosen for each participant. Each CRT block consisted of 40 stimuli, 20 for the fast and 20 for the slow condition, with randomly chosen stimuli out of the two response categories. In the figural (symmetry) task, stimuli were either the upper or lower two lines to the left and right of the “calculator 8” (symmetric condition), or the two possible combinations of one upper and one lower line at the left and right (asymmetric condition). In the numerical (odd–even) task, stimuli were “3”, “5”, and “7”, for the odd and “2”, “4”, and “6” for the even condition. In the verbal (consonant–vowel) task, stimuli were “F”, “H”, and “P” for the consonant and “A”, “E”, and “U” for the vowel condition.

#### 1.2.8. Perceptual speed: Comparison tasks

In the figural comparison task, two “fribbles”, coloured three-dimensional objects consisting of several connected parts, were shown to the left and right of the screen and participants had to decide as quickly as possible whether both objects were exactly the same or different. If different, objects differed only by one part. Images of fribbles used in this task are courtesy of Michael J. Tarr, Brown University, <http://www.tarrlab.org/>. In the numerical comparison task, two strings of five numbers each appeared to the left and right of the screen and participants had to decide as quickly as possible whether both strings were exactly the same or different. If different, strings differed only by one number. Number strings were randomly

assembled using digits 1–9. In the verbal comparison task, two strings of five letters each appeared to the left and right of the screen and participants had to decide as quickly as possible whether both strings were exactly the same or different. If different, strings differed only by one letter. Letters were lower case and randomly assembled from all consonants of the alphabet, precluding the possibility that they combined to real words. In each session, two blocks of 40 items were included for each comparison task, with equal numbers of same and different combinations.

### 1.3. Magnetic-resonance imaging (MRI) acquisition

At pretest and posttest, magnetic resonance images were acquired using a GE Signa LX 1.5-T system (General Electric, Milwaukee, WI) with actively shielded magnetic field gradients (maximum amplitude 40 m Tm<sup>-1</sup>). The MR protocol included a T1-weighted sagittal 3D scan (contrast-optimized spoiled gradient-echo sequence, 124 slices, slice thickness = 1.5 mm, FOV 250 mm × 250 mm; 256 × 256 matrix; TE = 8 ms; TR = 24 ms; flip angle = 30°) and a single-shot diffusion-weighted spin-echo-refocused echoplanar imaging sequence (FOV 280 mm × 280 mm; 128 × 128 matrix interpolated to 256 × 256; TE = 70 ms; TR = 10000 ms; 39 slices; slice thickness 3 mm; b-value 1000 s/mm<sup>2</sup>). The data for diffusion tensor calculations were collected with 12 non-collinear gradient orientations, each additionally measured with the opposite diffusion gradient polarity. The orientations were chosen according to the DTI acquisition scheme proposed by Papadakis, Xing, Huang, Hall, and Carpenter (1999). The total of 24 diffusion-weighted measurements, each an average of four measurements, were divided into four blocks, each preceded by a non-diffusion-weighted acquisition.

### 1.4. DTI analyses

The diffusion tensor images were eddy-current corrected (Bodammer, Kaufmann, Kanowski, & Tempelmann, 2004) and then corrected for head motion based on the non-diffusion-weighted images (Woods, Grafton, Holmes, Cherry, & Mazziotta, 1998). Diffusion tensors were calculated for each voxel and further decomposed into eigenvalues and eigenvectors. On the basis of the eigenvalues, mean diffusivity (MD) and fractional anisotropy (FA) maps were computed. For secondary analyses, we also computed maps displaying the axial and the radial diffusivity components, which reflect the diffusivity along the principal axis (i.e., longitudinal or parallel diffusivity) and the diffusivities of the two minor axes (i.e., perpendicular diffusivity), respectively. Each of these maps were visually inspected for imaging artifacts (e.g., movement, susceptibility artifacts).

After exact sagittal alignment of the diffusion tensor data and coregistration of pretest and posttest images (with nearest-neighbor assignment) a semi-automated segmentation of the corpus callosum (CC) was performed using the algorithm described by Niogi et al. (2007) implemented in Matlab (Mathworks Inc., Natick, MA). This approach classifies voxels as potentially being part of the CC dependent on the voxels' principal diffusion direction in combination with the voxel-inherent FA. This segmentation step was visually inspected by one operator to avoid that voxels were erroneously classified as belonging to the CC. For this purpose, we modified Niogi and colleagues' algorithm slightly. In our implementation, groups of connected CC candidate voxels form clusters, from which the operator selects those that constitute the CC. Only voxels selected for both the pretest and the posttest dataset (the intersection) were used for further analysis, which reduces partial volume effects and minimizes potential confounds with volume changes. The voxels obtained from nine consecutive midsagittal slices were then automatically subdivided into five segments by applying the geometric scheme presented by Hofer and Frahm (2006; Fig. 1A). These segments were shown by Hofer and Frahm (2006) to reliably distinguish between tracts connecting the prefrontal (segment 1), premotor and supplementary motor (2), motor (3), sensory (4), and temporal, parietal, and occipital cortices (5). Mean pretest and posttest values of MD, FA, and also axial and radial diffusivity were extracted from all CC partitions for each participant and time point. The test–retest (pretest–posttest) Pearson correlations of these measures were high for segment 1 ( genu:  $r_{FA} = 0.81$ ;  $r_{MD} = 0.87$ ;  $r_{axial} = 0.88$ ;  $r_{radial} = 0.83$ ) and segment 5 (splenium;  $r_{FA} = 0.80$ ;  $r_{MD} = 0.60$ ;  $r_{axial} = 0.71$ ;  $r_{radial} = 0.73$ ), indicating high stability and reliability of these measures. The correlations for the other three segments were lower (segment 2:  $r_{FA} = 0.67$ ;  $r_{MD} = 0.37$ ;  $r_{axial} = 0.50$ ;  $r_{radial} = 0.27$ ; segment 3:  $r_{FA} = 0.40$ ;  $r_{MD} = 0.23$ ;  $r_{axial} = 0.34$ ;  $r_{radial} = 0.02$ ; segment 4:  $r_{FA} = 0.64$ ;  $r_{MD} = 0.20$ ;  $r_{axial} = 0.41$ ;  $r_{radial} = 0.01$ ), presumably due to the smaller regions of interest. Thus, the trustworthiness of the segment 1 and segment 5 measures is high, whereas statistical power will be lower for segments 2–4 due to the lower stability and/or reliability of the measures from these segments, and the results for these segments should thus be interpreted with caution.

### 1.5. Segmentation of T1 MRI data

To assess the midsagittal area of the CC, a single operator manually aligned the T1-weighted 3D dataset exactly along the interhemispheric fissure and then manually segmented CC on the midsagittal slice. For all data sets the operator was blinded to the time of assessment and group status. The voxels obtained from the midsagittal slice were then automatically subdivided into the five partitions by applying the geometric scheme used for the DTI analyses (Hofer & Frahm, 2006; Fig. 1A). The test–retest correlations for these measures were all above 0.88, indicating high stability and reliability of these measures.

**Table 1**  
Mean diffusivity (mean and standard deviation in mm<sup>2</sup>/s) as a function of corpus callosum segment, time of assessment, and experimental group.

Segment	Younger intervention				Younger control				Older intervention				Older control			
	Pretest		Posttest		Pretest		Posttest		Pretest		Posttest		Pretest		Posttest	
	M	SD	M	SD	M	SD	M	SD	M	SD	M	SD	M	SD	M	SD
1	0.863	0.026	0.853	0.034	0.858	0.026	0.859	0.030	0.877	0.045	0.861	0.043	0.908	0.051	0.906	0.046
2	0.922	0.083	0.900	0.075	0.921	0.102	0.901	0.068	0.940	0.093	0.935	0.060	0.960	0.096	1.013	0.079
3	0.911	0.101	0.939	0.132	0.907	0.082	0.918	0.078	0.929	0.090	0.933	0.072	0.934	0.115	1.018	0.110
4	0.950	0.097	0.995	0.131	0.975	0.127	0.994	0.106	1.025	0.154	1.027	0.109	1.005	0.118	1.047	0.084
5	0.855	0.032	0.865	0.031	0.856	0.028	0.869	0.030	0.886	0.035	0.894	0.031	0.874	0.034	0.877	0.035

**Table 2**  
Mean fractional anisotropy (mean and standard deviation) as a function of corpus callosum segment, time of assessment, and experimental group.

Segment	Younger intervention				Younger control				Older intervention				Older control			
	Pretest		Posttest		Pretest		Posttest		Pretest		Posttest		Pre-test		Posttest	
	M	SD	M	SD	M	SD	M	SD	M	SD	M	SD	M	SD	M	SD
1	0.700	0.019	0.708	0.027	0.700	0.045	0.701	0.044	0.655	0.022	0.670	0.026	0.673	0.028	0.667	0.029
2	0.628	0.038	0.626	0.048	0.627	0.053	0.623	0.060	0.600	0.042	0.617	0.029	0.603	0.049	0.604	0.044
3	0.643	0.051	0.627	0.060	0.635	0.049	0.621	0.059	0.609	0.042	0.634	0.032	0.625	0.068	0.610	0.054
4	0.605	0.063	0.604	0.050	0.575	0.063	0.580	0.046	0.569	0.056	0.593	0.055	0.598	0.051	0.582	0.051
5	0.703	0.027	0.702	0.029	0.696	0.020	0.700	0.022	0.686	0.033	0.690	0.028	0.692	0.032	0.688	0.032

1.6. Statistical analyses

The inclusion of control groups enables dissociation of true intervention-related changes from confounding changes, such as maturation, aging-related decline, and time-of-year effects. With a control-group design, the critical intervention effect is revealed by an interaction between time of assessment (pretest vs. posttest) and experimental group (intervention vs. control); that is, changes between pretest and posttest for intervention groups that are significantly different from those for control groups. Similarly, age-related differences in intervention effects are revealed by an interaction between age group, time of assessment, and experimental group. To address these effects, we performed a series of univariate 2 (time; pretest vs. posttest) × 2 (experimental group; intervention vs. control) × 2 (age group; young vs. old) mixed analyses of variance (ANOVAs) separately for mean MD and FA of each of the five corpus callosum segments. These analyses were followed up with paired *t*-tests to probe the significance of the changes for each group separately. The threshold for significance was 0.05.

To maximize reliability of the cognitive data, we computed unit-weighted composites of the tasks measuring each cognitive ability. Each measure was first *z*-transformed using the means and standard deviations of the total sample at pretest as reference, so that age and time differences were preserved. Next the individual measures of working memory (three tasks), episodic memory (three tasks), and perceptual speed (six tasks) were averaged to form the three composites. Because the cognitive data were only available for the intervention groups, we analyzed performance for these groups with a series of univariate 2 (time; pretest vs. posttest) × 2 (age group; young vs. old) mixed analyses of variance (ANOVAs) separately for the three cognitive composites. For the corpus callosum segments displaying significant intervention-related mean changes, we additionally correlated changes in performance (i.e., difference scores; posttest–pretest), as indexed by the cognitive composites, with changes in FA and MD. Partial correlations were computed with the two age groups collapsed, controlling for the influence of age. The threshold for significance (0.05) was corrected for multiple comparisons.

2. Results

Results from ANOVAs applied to the primary DTI data (Fig. 1, Tables 1 and 2) revealed intervention-related change in the form

of an interaction between experimental group (intervention vs. control) and time (pretest vs. posttest) for MD (Fig. 1B) in segment 1 (genu) of the corpus callosum,  $F(1,51)=4.40, p=0.041$ . MD decreased in both the younger,  $t(19)=2.57, p=0.019$ , and the older intervention group,  $t(11)=2.39, p=0.036$ . The control groups showed no significant changes, both  $ts < 0.21$ . FA (Fig. 1C) displayed a similar pattern of intervention-related change in segment 1,  $F(1,51)=6.08, p=0.017$ . The older intervention group increased significantly in FA,  $t(11)=3.12, p=0.010$ , but the increase for the younger intervention group did not reach significance,  $t(19)=1.64$ . The control groups showed no significant changes,  $ts < 1.22$ . The main effect of age reached significance for both MD,  $F(1,51)=8.49, p=0.005$ , and FA,  $F(1,51)=22.06, p < 0.001$ . MD increased and FA decreased with age (see Tables 1 and 2). No other effects reached significance. Note especially that the age by experimental group by time interaction were neither significant for MD nor for FA, both  $Fs(1,51) < 1.84$ , indicating that the intervention-related effect did not differ significantly between age groups. Note also that the main effect of experimental group was not significant, and that additional univariate ANOVAs on pretest FA- and MD-values at pretest showed no significant effect of experimental group [both  $Fs(1,51) < 1.5$ ], indicating the experimental groups were comparable on the primary DTI data at baseline. No other segment displayed significant intervention-related change,  $Fs(1,51) < 1.75$ .

To explicitly examine the potential regional selectivity of the intervention-related effect observed in the genu, we conducted additional ANOVAs including segment as a two-level factor (segment 1 vs. segment 5). Segment 5 (i.e., the splenium) was chosen as the control region in these analyses because its' similar size and overall comparable reliability of the FA and MD measures with seg-

**Table 3**  
Mean cognitive performance on trained tasks as a function of age group and time.

Measure	Younger intervention				Older intervention			
	Pretest		Posttest		Pretest		Posttest	
	M	SD	M	SD	M	SD	M	SD
Working memory	0.46	0.63	1.57	0.82	-0.77	0.49	0.52	0.61
Episodic memory	0.34	0.89	1.44	1.20	-0.57	0.46	0.05	0.95
Perceptual speed	0.29	0.57	1.62	0.67	-0.49	0.55	0.30	0.80

Note: The measures are averages of *z*-standardized (using the *M* and *SD* of the total sample at pretest) individual measures of working memory (three tasks), episodic memory (three tasks), and perceptual speed (six tasks), respectively.

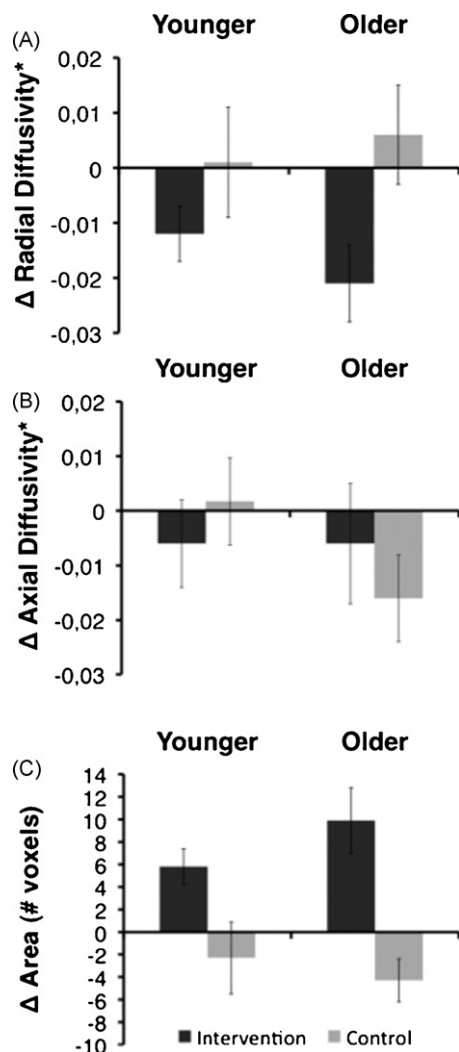


**Fig. 2.** Mean change ( $\Delta$ ;  $\pm$ SE) from pretest to posttest in (A) radial diffusivity, (B) axial diffusivity, and (C) area (number of voxels) of segment 1 (genu) of the corpus callosum as a function of age and experimental group.

ment 1 (i.e., the genu). In these analyses, the effect of interest is the experimental group by time by segment interaction, which picks up differences in intervention-related changes between the segments. There was a non-significant trend for such an effect for FA,  $F(1,51)=3.23$ ,  $p=0.078$ , and a non-significant result for MD,  $F(1,51)=1.48$ ,  $p=0.229$ .

Cognitive performance (see Table 3) increased over time for working memory,  $F(1,30)=199.44$ ,  $p<0.001$ , episodic memory,  $F(1,30)=59.54$ ,  $p<0.001$ , and perceptual speed,  $F(1,30)=121.40$ ,  $p<0.001$ . Younger adults had higher scores on all cognitive composites, working memory,  $F(1,30)=24.47$ ,  $p<0.001$ , episodic memory,  $F(1,30)=12.28$ ,  $p<0.001$ , and perceptual speed,  $F(1,30)=23.37$ ,  $p<0.001$ . The age group by time interaction reached significance for perceptual speed,  $F(1,30)=7.69$ ,  $p=0.009$ , and episodic memory,  $F(1,30)=4.68$ ,  $p=0.039$ , indicating larger increases over time for younger relative to older adults. No other effects were significant.

Next, we correlated changes in performance on the working memory, episodic memory, and perceptual speed composites with changes in FA and MD. We focused on segment 1 because this region showed significant intervention-related change. We included both younger and older adults that took part in training and partialled for the influence of age. None of the correlations reached significance (all  $ps>0.21$ ).

Finally, to further probe the observed changes in segment 1, we performed secondary analyses of radial and axial diffusivity. Here, the ANOVAs revealed a significant intervention-related decrease in radial (Fig. 2A),  $F(1,51)=6.60$ ,  $p=0.013$ , but not in axial (Fig. 2B),  $F(1,51)<0.03$ , diffusivity. In addition, we observed significant intervention-related increase for the midsagittal area of segment 1 (Fig. 2C) on structural high-resolution images,  $F(1,51)=22.88$ ,  $p<0.001$ .

### 3. Discussion

This study shows that white-matter microstructure, as indexed by FA and MD obtained from the anterior part of the corpus callosum, is modifiable by experience in both younger and older adulthood. These results add validity to evidence of experience-dependent plasticity of white matter in early adulthood (e.g., Fields, 2008; Scholz et al., 2009) and reveal that such plasticity extends into old age, thereby clearly demonstrating that experience can change white-matter microstructure well beyond periods of the lifespan during which maturational myelination occurs. Most of the cognitive tasks that we used to induce experience-related white-matter changes are known to involve the prefrontal cortices (Cabeza & Nyberg, 2000) and demand attentional control that requires interhemispheric communication (Banich, 1998; Mikels & Reuter-Lorenz, 2004). Though other brain regions are also activated by the trained tasks, it is likely that the treatment we leveraged, which was massive in terms of the range of administered tasks and intensiveness, induced these changes. In addition, factors such as the increased social stimulation due to the extensive training procedure may have contributed to the observed effects. Regardless of the relative contribution of these factors, our findings lead to the novel conclusion that experience-dependent plasticity of white-matter microstructure is also present in later adulthood. Whether such plasticity is restricted to relatively healthy young–old (65–75-year old) adults, constituting the sample in this study, or whether plasticity of white-matter also extends into very old age is a topic for future research.

Though great care should be taken when linking observed changes in DTI metrics to potential histological changes (e.g., Wheeler-Kingschott & Cercignani, 2009), our secondary analyses of radial (i.e., perpendicular) and axial (i.e., parallel) diffusivity of the most anterior segment of corpus callosum reveal an intriguing pattern of changes in radial, but not in axial, diffusivity – a pattern that has been linked to myelination (Alexander, Lee, Lazar, & Field, 2007; Song et al., 2005). In addition, we observed significant intervention-related area increase for this segment. This finding argues against dehydration as a cause of the observed diffusivity changes. The possibility that experience may induce an increase in myelination is well compatible with the observation that myelination is not static across adulthood. Rather, there is complex and ongoing dynamics of demyelination and myelination across adulthood (Bartzokis, 2009; Wozniak & Lim, 2006), possibly pointing to a persistent potential for experience-dependent plasticity.

We note that the analyses did not detect any significant age-related differences in plasticity of white-matter microstructure, which contrasts with reports of age-related decline in training-related improvements in cognitive performance (e.g., Kliegl, Smith, & Baltes, 1989), functional brain activity (Lustig, Shah, Seidler, & Reuter-Lorenz, 2009), and gray matter structure (Boyke, Driemeyer, Gaser, Buchel, & May, 2008). Though the relatively small sample size in this study limits the power to detect such age interactions, we note that the older adults in this study, if anything, displayed numerically larger intervention-related increases than younger adults (see Fig. 1, Tables 1 and 2). In this vein, we also highlight that the absence of intervention-related effects in segments

2–4 (i.e., the body of the corpus callosum) should be interpreted with caution, considering the low reliabilities of the DTI measures in these segments. The absence of significantly larger intervention-related changes in segment 1 as compared with segment 5 also limit inferences of regional selectivity of the observed effects. However, we hasten to add that we observed a non-significant trend for such an effect for FA and that null-findings should not be overinterpreted considering the limited power of the study to detect such interactions.

Our findings of experience-dependent plasticity of white-matter microstructure inform research on several disorders (e.g., schizophrenia and late-onset Alzheimer's disease) in which disrupted connectivity is a major cause for dysfunction (Bartzokis, 2009; Feng, 2008; Fields, 2008) and are particularly applicable to aging-related cognitive decline. White-matter microstructure in the genu is linked to cognitive decline in aging (Madden, Spaniol, et al., 2009) and to increases of activation in the prefrontal cortices during cognitive tasks (Persson et al., 2006). These age-related functional differences might partially be accounted for by reductions in the efficiency of inter-hemispheric communication (O'Sullivan et al., 2001; Sullivan & Pfefferbaum, 2006) and disruption of synchronous operation of brain networks (Andrews-Hanna et al., 2007), stemming from age-related white-matter degradation (Sullivan & Pfefferbaum, 2006). Though we did not detect any significant associations between altered white-matter microstructure and improvements in cognitive performance in this study, which is not surprising considering the potentially low reliability of raw difference scores and the limited sample size for analyzing between-person differences, our findings open new opportunities for future studies to address how improved white-matter microstructure might enhance such neural processes. That is, the discovery of experience-dependent plasticity of white-matter microstructure in later human adulthood adds promise to attempts to attenuate cognitive impairments in aging.

### Conflicts of interest

None declared.

### Acknowledgements

Funded by the Max Planck Institute for Human Development, the Innovation Fund of the Max Planck Society, the Sofja Kovalevskaja Award (to ML) administered by the Alexander von Humboldt Foundation and donated by the German Federal Ministry for Education and Research (BMBF), Deutsche Forschungsgemeinschaft, and the BMBF. We thank Colin Bauer, Annette Brose, Christian Chicherio, and all research assistants.

### References

- Alexander, A. L., Lee, J. E., Lazar, M., & Field, A. S. (2007). Diffusion tensor imaging of the brain. *Neurotherapeutics*, 4(3), 316–329.
- Andrews-Hanna, J. R., Snyder, A. Z., Vincent, J. L., Lustig, C., Head, D., Raichle, M. E., et al. (2007). Disruption of large-scale brain systems in advanced aging. *Neuron*, 56(5), 924–935.
- Banich, M. T. (1998). The missing link: The role of interhemispheric interaction in attentional processing. *Brain and Cognition*, 36(2), 128–157.
- Bartzokis, G. (2009). Alzheimer's disease as homeostatic responses to age-related myelin breakdown. *Neurobiology of Aging*.
- Bengtsson, S. L., Nagy, Z., Skare, S., Forsman, L., Forssberg, H., & Ullen, F. (2005). Extensive piano practicing has regionally specific effects on white matter development. *Nature Neuroscience*, 8(9), 1148–1150.
- Bodammer, N., Kaufmann, J., Kanowski, M., & Tempelmann, C. (2004). Eddy current correction in diffusion-weighted imaging using pairs of images acquired with opposite diffusion gradient polarity. *Magnetic Resonance in Medicine*, 51(1), 188–193.
- Boyke, J., Driemeyer, J., Gaser, C., Buchel, C., & May, A. (2008). Training-induced brain structure changes in the elderly. *Journal of Neuroscience*, 28(28), 7031–7035.
- Burzynska, A. Z., Preuschhof, C., Backman, L., Nyberg, L., Li, S. C., Lindenberger, U., et al. (2010). Age-related differences in white matter microstructure: region-specific patterns of diffusivity. *Neuroimage*, 49(3), 2104–2112.
- Cabeza, R., & Nyberg, L. (2000). Imaging cognition II: An empirical review of 275 PET and fMRI studies. *Journal of Cognitive Neuroscience*, 12(1), 1–47.
- Demerens, C., Stankoff, B., Logak, M., Anglade, P., Allinquant, B., Couraud, F., et al. (1996). Induction of myelination in the central nervous system by electrical activity. *Proceedings of the National Academy of Sciences of the United States of America*, 93(18), 9887–9892.
- Feng, Y. (2008). Convergence and divergence in the etiology of myelin impairment in psychiatric disorders and drug addiction. *Neurochemical Research*, 33(10), 1940–1949.
- Fields, R. D. (2008). White matter in learning, cognition and psychiatric disorders. *Trends in Neurosciences*, 31(7), 361–370.
- Folstein, M. F., Folstein, S. E., & McHugh, P. R. (1975). "Mini-mental state": A practical method for grading the cognitive state of patients for the clinician. *Journal of Psychiatric Research*, 12(3), 189–198.
- Hofer, S., & Frahm, J. (2006). Topography of the human corpus callosum revisited – comprehensive fiber tractography using diffusion tensor magnetic resonance imaging. *Neuroimage*, 32(3), 989–994.
- Kliegl, R., Smith, J., & Baltes, P. B. (1989). Testing-the-limits and the study of adult age-differences in cognitive plasticity of a mnemonic skill. *Developmental Psychology*, 25(2), 247–256.
- Lehrl, S., Merz, J., Burkard, G., & Fischer, B. (1991). *Manual zum MWT-A [manual for MWT-A]*. Erlangen, Germany: Perimed.
- Lindenberger, U., Mayr, U., & Kliegl, R. (1993). Speed and intelligence in old age. *Psychology and Aging*, 8(2), 207–220.
- Lustig, C., Shah, P., Seidler, R., & Reuter-Lorenz, P. A. (2009). Aging, training, and the brain: A review and future directions. *Neuropsychology Review*, 19(4), 504–522.
- Madden, D. J., Bennett, I. J., & Song, A. W. (2009). Cerebral white matter integrity and cognitive aging: Contributions from diffusion tensor imaging. *Neuropsychology Review*, 19(4), 415–435.
- Madden, D. J., Spaniol, J., Costello, M. C., Bucur, B., White, L. E., Cabeza, R., et al. (2009). Cerebral white matter integrity mediates adult age differences in cognitive performance. *Journal of Cognitive Neuroscience*, 21(2), 289–302.
- Mikels, J. A., & Reuter-Lorenz, P. A. (2004). Neural gate keeping: the role of interhemispheric interactions in resource allocation and selective filtering. *Neuropsychology*, 18(2), 328–339.
- Niogi, S. N., Mukherjee, P., & McEandliss, B. D. (2007). Diffusion tensor imaging segmentation of white matter structures using a reproducible objective quantification scheme (ROQS). *NeuroImage*, 35, 166–174.
- O'Sullivan, M., Jones, D. K., Summers, P. E., Morris, R. G., Williams, S. C., & Markus, H. S. (2001). Evidence for cortical "disconnection" as a mechanism of age-related cognitive decline. *Neurology*, 57(4), 632–638.
- Papadakis, N. G., Xing, D., Huang, C. L., Hall, L. D., & Carpenter, T. A. (1999). A comparative study of acquisition schemes for diffusion tensor imaging using MRI. *Journal of Magnetic Resonance*, 137(1), 67–82.
- Persson, J., Nyberg, L., Lind, J., Larsson, A., Nilsson, L. G., Ingvar, M., et al. (2006). Structure–function correlates of cognitive decline in aging. *Cerebral Cortex*, 16(7), 907–915.
- Sanchez, M. M., Hearn, E. F., Do, D., Rilling, J. K., & Herndon, J. G. (1998). Differential rearing affects corpus callosum size and cognitive function of rhesus monkeys. *Brain Research*, 812(1–2), 38–49.
- Schmiedek, F., Lövdén, M., & Lindenberger, U. (2010). Hundred days of cognitive training enhance broad cognitive abilities in adulthood: Findings from the COGITO study. *Frontiers in Aging Neuroscience*, 2, 1–10.
- Scholz, J., Klein, M. C., Behrens, T. E., & Johansen-Berg, H. (2009). Training induces changes in white-matter architecture. *Nature Neuroscience*, 12(11), 1370–1371.
- Song, S. K., Yoshino, J., Le, T. Q., Lin, S. J., Sun, S. W., Cross, A. H., et al. (2005). Demyelination increases radial diffusivity in corpus callosum of mouse brain. *Neuroimage*, 26(1), 132–140.
- Stevens, B., Porta, S., Haak, L. L., Gallo, V., & Fields, R. D. (2002). Adenosine: A neuron–glial transmitter promoting myelination in the CNS in response to action potentials. *Neuron*, 36(5), 855–868.
- Sullivan, E. V., & Pfefferbaum, A. (2006). Diffusion tensor imaging and aging. *Neuroscience and Biobehavioral Reviews*, 30(6), 749–761.
- Wheeler-Kingschott, C. A., & Cercignani, M. (2009). About "axial" and "radial" diffusivities. *Magnetic Resonance in Medicine*, 61, 1255–1260.
- Woods, R. P., Grafton, S. T., Holmes, C. J., Cherry, S. R., & Mazziotta, J. C. (1998). Automated image registration: I. General methods and intrasubject, intramodality validation. *Journal of Computer Assisted Tomography*, 22(1), 139–152.
- Wozniak, J. R., & Lim, K. O. (2006). Advances in white matter imaging: A review of in vivo magnetic resonance methodologies and their applicability to the study of development and aging. *Neuroscience and Biobehavioral Reviews*, 30(6), 762–774.